

# Establishing baselines for generative discovery of inorganic crystals

Nathan J. Szymanski<sup>1</sup> and Christopher J. Bartel<sup>1,\*</sup>

## Abstract

Generative artificial intelligence offers a promising avenue for materials discovery, yet its advantages over traditional methods remain unclear. In this work, we introduce and benchmark two baseline approaches – random enumeration of charge-balanced prototypes and data-driven ion exchange of known compounds – against three generative models: a variational autoencoder, a large language model, and a diffusion model. Our results show that established methods such as ion exchange perform comparably well in generating stable materials, although many of these materials tend to closely resemble known compounds. In contrast, generative models excel at proposing novel structural frameworks and, when sufficient training data is available, can more effectively target properties such as electronic band gap and bulk modulus while maintaining a high stability rate. To enhance the performance of both the baseline and generative approaches, we implement a post-generation screening step in which all proposed structures are passed through stability and property filters from pre-trained machine learning models including universal interatomic potentials. This low-cost filtering step leads to substantial improvement in the success rates of all methods, remains computationally efficient, and ultimately provides a practical pathway toward more effective generative strategies for materials discovery.

---

<sup>1</sup> University of Minnesota, Department of Chemical Engineering and Materials Science, Minneapolis, MN, USA 55455

\* Correspondence to [cbartel@umn.edu](mailto:cbartel@umn.edu)

## Introduction

The discovery of new materials has long been a cornerstone of technological progress, driving many of the innovations that shape modern society.<sup>1</sup> Breakthroughs in layered and Li-rich battery cathodes, for example, have enabled the widespread adoption of portable electronics and electric vehicles.<sup>2</sup> Transparent conducting oxides such as indium tin oxide (ITO) and indium gallium zinc oxide (IGZO) have been critical for the development of touch screens, solar cells, and flat-panel displays.<sup>3</sup> Similarly, the discovery of cuprate superconductors in the 1980s reignited interest in high-temperature superconductivity, which remains the subject of extensive research.<sup>4</sup> These examples highlight the role of materials discovery in advancing transformative technologies and underscore the need for innovative approaches to accelerate future breakthroughs.

The recent emergence of generative artificial intelligence (AI) offers a promising route for designing new materials, particularly inorganic crystals.<sup>5</sup> Early efforts focused on generative adversarial networks (GANs)<sup>6–8</sup> and variational autoencoders (VAEs),<sup>9–13</sup> while more recent developments include large language models (LLMs)<sup>14–16</sup>, diffusion-based techniques,<sup>17–20</sup> and normalizing flows.<sup>21,22</sup> These generative models are often trained on computed materials from open databases such as the Materials Project<sup>23</sup> to generate thermodynamically stable structures, with some also conditioned on specific properties for application-driven campaigns.

Despite the rapid growth in generative models, it remains difficult to systematically assess their performance in a consistent fashion. Tools like *matbench-genmetrics* provide important frameworks and metrics for evaluating the validity of structures proposed by generative models,<sup>24</sup> while *matbench-discovery* addresses the challenge of benchmarking stability predictions made by machine learning (ML) models and interatomic potentials.<sup>25</sup> Yet, the extent to which generative models outperform established methods, such as ion exchange or high-throughput screening, is not yet fully understood. Baselines are therefore essential to clarify where these models offer the greatest advantages – whether in producing stable materials, generating novel structures, or achieving targeted properties – and to identify their limitations. Such benchmarks are key to integrating generative models into existing workflows and driving tangible progress in materials discovery.

In this work, we establish two baseline methods for the generation of inorganic crystals: random enumeration of charge-balanced chemical formulae in structure prototypes sourced from the AFLOW database,<sup>26,27</sup> and ion exchange of stable compounds with desired properties from the

Materials Project.<sup>23</sup> These methods are benchmarked against three generative models – CrystaLLM,<sup>14</sup> FTCP,<sup>11</sup> and CDVAE<sup>12</sup> – for the generation of (1) materials that are stable and novel, (2) materials with a band gap near 3 eV, and (3) materials with high bulk modulus. We also integrate two graph neural networks, CHGNet<sup>28</sup> and CGCNN,<sup>29</sup> to filter and retain generated materials predicted to be stable or exhibit desired properties. This evaluation sheds light on the comparative strengths and weaknesses of traditional and generative approaches to materials discovery, while also providing a set of baselines against which future generative models can be benchmarked.

## Methods

### Random enumeration

In this method, we randomly paired a known structure prototype with a set of elements also chosen at random. The prototypes were drawn from 1,783 structures listed in the Encyclopedia of Crystallographic Prototypes (AFLOW).<sup>26,27</sup> Compositional sets were created using three to five elements, forming ternary to quinary phases. Binary phases were excluded because they have been extensively studied already, leaving little opportunity for novel materials discovery. For each structure-composition pair, we assigned the elements to specific prototype sites based on the given chemical formula. For example, randomly selecting the prototype “A2BC4\_cF56\_227\_c\_b\_e-001” (a normal spinel in the AFLOW prototype library) and a composition of Mn-Fe-S would yield six spinel structures by exploring all possible arrangements of Mn, Fe, and S on the *A/B/C* sites. Charge balance is then assessed using common oxidation states provided by *pymatgen*.<sup>30</sup> If charge balance is plausible, the structure of the prototype is decorated accordingly, and the resulting materials undergo further evaluation using density functional theory (DFT). In the previous example, only Mn<sub>2</sub>FeS<sub>4</sub> and Fe<sub>2</sub>MnS<sub>4</sub> would be retained of the six enumerated structures.

### Data-driven ion exchange

The Materials Project (MP) contains DFT-calculated properties for ~153,000 compounds, providing a solid foundation for materials discovery campaigns.<sup>23</sup> Starting from these materials, we leveraged the data-mined substitution prediction (DMSP) algorithm<sup>31</sup> implemented in *pymatgen*<sup>30</sup> to replace one or more ions of a given compound to yield new hypothetical materials. The substitutions are guided by conditional probabilities,  $p_{\text{DMSP}}$ , which quantify the likelihood of

substituting one ion for another while retaining the original crystal structure. These probabilities are derived from a probabilistic model trained on the Inorganic Crystal Structure Database (ICSD), an experimental database of known crystal structures.<sup>32</sup> Substitutions were performed for pairs of species with  $p_{\text{DMSP}} > 0.001$  (the default value in *pymatgen*) to balance the tradeoff between generating novel substitutions and maintaining structural plausibility. Multiple substitutions were allowed per material, enabling both single and multi-site exchanges. For example, starting from  $\text{CaTiO}_3$  yields substitutions like  $\text{SrTiO}_3$  and  $\text{SrZrO}_3$  (single-site), in addition to  $\text{SrTiS}_3$  and  $\text{SrZrS}_3$  (multi-site). DMSP was applied in two different modes: 1) to generate stable materials and 2) to generate materials with desired properties. For the first task, we randomly extracted stable parent structures from MP and substituted at least one ion with a species not already present in the original composition. To generate materials with desired properties, we selected materials having specified target values of that property (*e.g.*, band gaps near 3 eV) and performed ion substitution in a similar fashion to generate new structures.

## Generative modeling

Three generative models were tested in this work, each trained on a dataset of 45,231 stable inorganic crystals (denoted MP-20)<sup>12</sup> from the Materials Project. The first (CrystaLLM)<sup>14</sup> is a transformer-based large-language model designed to learn from tokenized representations of CIF files. We used a pre-configured version of the model (from [github.com/lantunes/CrystaLLM](https://github.com/lantunes/CrystaLLM)) that was trained on MP-20. The second model (FTCP)<sup>11</sup> encodes materials using real-space features, such as lattice vectors, one-hot encoded element vectors, site coordinates, and occupancies, in addition to reciprocal-space features derived from a Fourier transform of elemental property vectors. Two FTCP-based autoencoders were trained on the MP-20 dataset: one conditioned on formation energy and electronic band gap and another conditioned on formation energy and bulk modulus. Due to the limited availability of elastic property data, the latter autoencoder was trained and validated on a subset of MP-20 containing 9,361 materials. The third model (CDVAE)<sup>12</sup> combines a variational autoencoder with a diffusion model to generate new materials. Sampling from the latent space predicts composition, lattice vectors, and the number of atoms in the unit cell, which are used to randomly initialize structures. The diffusion component of the model then “de-noises” these random structures by iteratively perturbing atoms toward equilibrium positions.

We trained CDVAE on MP-20 without any conditioning of its latent space, allowing it to be used only for the generation of stable materials.

### Density functional theory calculations

A subset of the generated structures was relaxed using the PBE exchange-correlation functional<sup>33</sup> within the projector augmented wave (PAW) method as implemented in the Vienna *Ab Initio* Simulation Package (VASP).<sup>34,35</sup> These calculations used a plane-wave cutoff energy of 520 eV with a  $\Gamma$ -centered k-point grid spacing of 0.22  $\text{\AA}^{-1}$ . Convergence criteria were set to  $10^{-6}$  eV for the electronic optimizations and 0.03 eV/ $\text{\AA}$  for the ionic relaxations. Symmetry was turned off to ensure accurate treatment of distortions, and spin polarization was included for materials containing magnetic elements. Moments were initialized in a ferromagnetic configuration for all such compounds. For materials containing 3d transition metals, Hubbard U corrections (+U) were applied to account for on-site Coulomb interactions following the conventions used in the Materials Project: 4.0 eV for Mn, 3.9 eV for Fe, 3.7 eV for Co, 6.2 eV for Ni, and 5.3 eV for Cu.<sup>23</sup>

Thermodynamic stability with respect to all known competing phases in MP was evaluated using the decomposition energy ( $\Delta E_d$ ).<sup>36</sup> For unstable materials with  $\Delta E_d > 0$ , this measure is equivalent to the energy above the convex hull ( $E_{\text{hull}}$ ). It quantifies the energy difference between the proposed material and the lowest energy combination of competing phases. For stable materials with  $\Delta E_d \leq 0$ , the decomposition energy is the energy by which the proposed material lies below the existing convex hull (if the proposed material were not included in its construction). Total energies acquired from DFT calculations were transformed into formation energies ( $\Delta E_f$ ) using the *MaterialsProject2020* compatibility scheme, which accounts for GGA/GGA+U mixing and implements elemental reference energy corrections as described in previous work.<sup>37</sup> Competing phases were identified by constructing a phase diagram for each chemical system using the *PhaseDiagram* module from *pymatgen*.<sup>30</sup> For evaluating each approach to material generation, phase diagrams included all entries from MP (as of December 2024) as well as the generated entries themselves, allowing for an evaluation of stability against both known and hypothetical phases.

Electronic band gaps were computed by analyzing the eigenvalue band properties obtained from VASP calculations using *pymatgen*,<sup>30</sup> with the band gap defined as the energy difference between the valence band maximum and conduction band minimum. The bulk modulus of each

structure was computed by fitting a Birch-Murnaghan equation of state<sup>38</sup> to relaxed (but fixed volume) total energy calculations performed at seven volumes ranging from 97% to 103% of the equilibrium volume. These volumes were generated by isotropically scaling the lattice vectors of the relaxed equilibrium structures. The equilibrium bulk modulus and its pressure derivative were extracted from the fit, providing a measure of each material’s resistance to volumetric deformation.

### **Novelty assessment**

A material was considered novel if it was not already present in MP (as of December 2024), thus ensuring it was excluded from the training data used for the generative models evaluated here. To determine this, we queried all entries in MP with the same composition as a proposed structure. For each resulting entry, structural similarity was assessed using the *StructureMatcher* tool in *pymatgen*,<sup>30</sup> which compares structures based on their lattice parameters, atomic positions, and symmetry. We used loose tolerance parameters for this comparison to account for slight variations in computed structures. This included a lattice parameter tolerance of 0.25 Å, a site tolerance defined as 40% of the average free length per atom, and an angular tolerance of 10°. If no matching composition or structure was identified in the MP database, the phase was classified as novel.

### **Machine learning filtering**

Universal machine learning interatomic potentials (uMLIPs) offer an efficient way to screen large numbers of candidate materials obtained from any of the methods described above, enabling the rapid identification of promising structures prior to more computationally expensive DFT calculations. Here, we used CHGNet<sup>28</sup> to compute the internal (0 K) energies of all candidate materials, which were then compared against the convex hulls in MP to assess thermodynamic stability. Each structure was relaxed using the Atomic Simulation Environment (ASE)<sup>39</sup> with CHGNet-based force fields, ensuring the forces acting on its atoms converged below 0.1 eV/Å. This relatively loose convergence criterion was chosen to improve computational efficiency for the task of high-throughput screening. CHGNet was trained on GGA and GGA+U calculations with *MaterialsProject2020Compatibility* corrections applied,<sup>37</sup> enabling direct comparison with MP energies. Thermodynamic stability was evaluated by constructing phase diagrams for the relevant chemical systems, incorporating all MP entries (as of December 2024) alongside

generated candidate structures. Materials predicted to be stable within these phase diagrams were passed to DFT calculations for further validation.

For property-specific screening, we leveraged two pre-trained CGCNN<sup>29</sup> models: one trained on 16,458 DFT-calculated band gaps and the other on 2,041 bulk moduli from MP. When generating materials with a high bulk modulus, we applied an acceptance criterion of CGCNN-predicted bulk moduli exceeding 200 GPa. Analogously, when generating materials with a band gap near 3 eV, we selected candidates with CGCNN-predicted band gaps in the range of 2.8 to 3.2 eV.

## Results

### Stability and novelty

Each method described above was used to generate 500 distinct materials that were passed to DFT calculations. The distributions of decomposition energies ( $\Delta E_d$ ) for these materials relative to the convex hull defined by MP entries are shown in **Figure 1**. Random enumeration of known structure prototypes with charge-balanced chemical formulae produces a wide range of energies, with many materials lying far above the convex hull. About 4.3% of the materials obtained from this method are thermodynamically stable ( $\Delta E_d \leq 0$ ), which may seem low at first glance but is surprisingly high given the simplicity of random enumeration. Building on this approach, further improvement to the stability rate can be achieved by leveraging analogies to known materials. Data-driven ion exchange results in a significantly tighter distribution of energies closer to the convex hull, with 19.1% of the materials being thermodynamically stable. The success of this approach is impressive but perhaps unsurprising, given its proven efficacy in discovering new materials through high-throughput calculations over the past decade.<sup>40-44</sup>

CrystaLLM produces materials with the widest range of energies among the generative models, with only 1.4% of its generated materials being stable and a substantial 32.6% of them exhibiting  $\Delta E_d > 0.5$  eV/atom. This stability rate is lower than those of the baseline methods (random enumeration and ion exchange), likely in part because CrystaLLM does not incorporate known structural frameworks or enforce charge neutrality during generation. When we restrict the analysis to CrystaLLM-generated materials that (1) can be matched to a known structure prototype in AFLOW and (2) are charge-balanced, the stability rate increases slightly to 1.8%. This modest improvement suggests that while the lack of structural frameworks and charge neutrality

contributes to CrystaLLM’s lower stability rate, additional factors – possibly related to the challenge of learning stability from text alone – may also play a significant role.

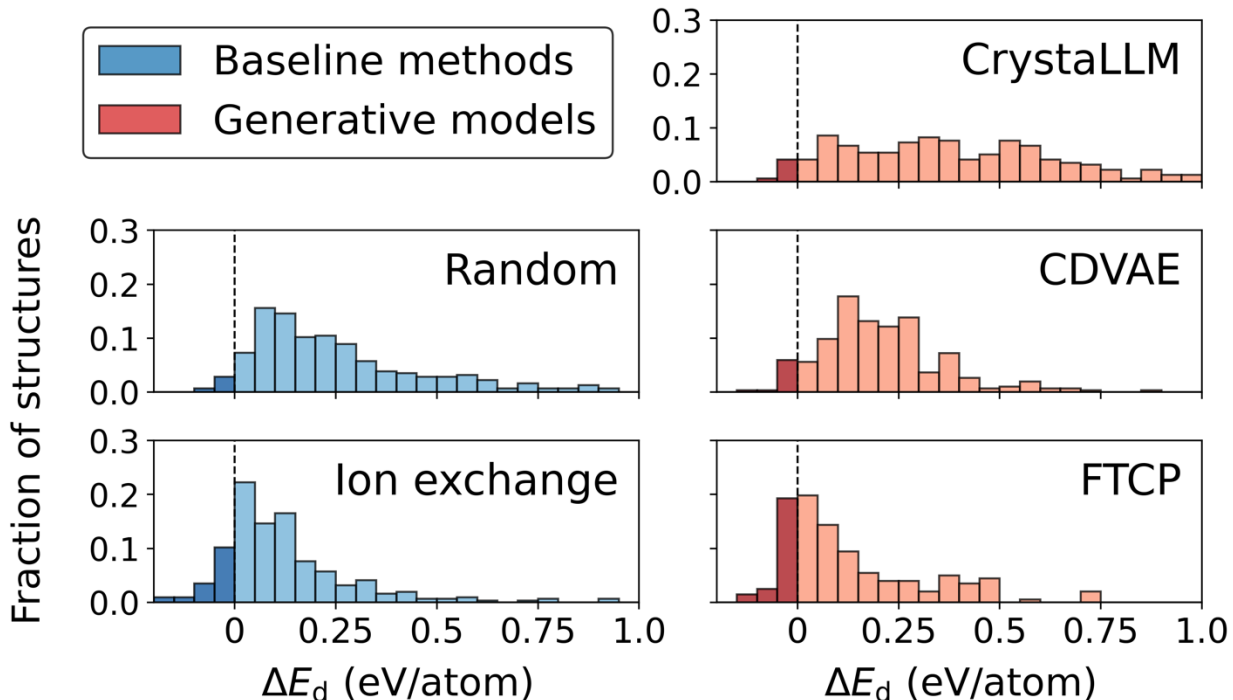


**Figure 1:** Histograms showing density functional theory (DFT) computed decomposition energies of structures generated by two baseline methods and three generative models. For each of the five approaches, 500 structures were considered. The left column (blue) contains results from the baseline methods: random enumeration and ion exchange. The right column (red) contains results from the generative model: CrystaLLM,<sup>14</sup> FTCP,<sup>11</sup> and CDVAE.<sup>12</sup>

Both FTCP and CDVAE substantially outperform CrystaLLM in generating stable materials, with stability rates of 26.8% and 6.3%, respectively. The superior performance of FTCP over CDVAE is somewhat unexpected, given the recent popularity of diffusion models like CDVAE for generative tasks. However, we speculate that FTCP’s advantage can be attributed to its latent space sampling strategy, which biases generation toward materials that are structurally similar to known stable compounds. This approach is likely to enhance the stability rate, similar to the observed benefits of reference-based strategies (data-driven ion exchange) in the baseline methods.



We next evaluate the novelty of materials proposed by each method. In the context of this work, novelty is defined as a material being absent from MP. While this does not necessarily indicate the material has never been synthesized or is absent from all other computational databases (such as OQMD<sup>45</sup> or NOMAD<sup>46</sup>), it signifies that the material was not used for training of the generative models or as a template for ion exchange. The novelty rate of each method is listed in **Table 1**, along with the  $S \cap N$  rate that defines the percentage of materials that are both stable *and* novel. Between the two baseline methods, random enumeration yields a much higher novelty rate (98.4%) than ion exchange (70.5%). This reflects the unconstrained nature of random enumeration, which leads to the sampling of many previously unexplored chemical compositions. In contrast, our approach to ion exchange closely reflects traditional screening efforts,<sup>47</sup> and is therefore more likely to reproduce materials already present in computational databases such as MP. However, the use of ion exchange also comes with the benefit of generating more stable materials, resulting in a higher  $S \cap N$  rate (7.4%) than random enumeration (3.8%).

**Table 1:** Stability and novelty rates of materials generated from each method. The  $S \cap N$  rate is the percentage of materials that are both stable and novel, where novelty is assessed based on the absence of a material from MP. Also listed is the prototype novelty rate, defined as the percentage of proposed materials whose structures cannot be indexed to a known prototype in the AFLOW database, and the stability rate of materials in these novel prototypes ( $S \cap N$ ). The bold value in each column denotes the highest rate achieved among all methods. Statistics are based on 500 structures generated by each method.

Method	Stability rate	Novelty rate	$S \cap N$ rate	Prototype novelty rate	Prototype $S \cap N$ rate
Random	4.3%	<b>98.4%</b>	3.8%	0%	0%
Ion exchange	19.1%	70.5%	<b>7.4%</b>	0%	0%
CrystaLLM	1.4%	91.5%	1.1%	6.4%	0%
CDVAE	6.3%	96.5%	4.8%	<b>16.5%</b>	0%
FTCP	<b>26.8%</b>	49.1%	5.6%	8.3%	0%

Among the generative models, CrystaLLM and CDVAE exhibit high novelty rates of 91.5% and 96.5%, respectively. In contrast, only about 49.1% of materials generated by FTCP are not already present in MP. The reduced novelty rate is consistent with FTCP’s strategy of sampling

around known materials in its latent space, a factor that likely also contributes to its higher stability rate. Despite FTCP achieving a significantly higher stability rate than CDVAE, the two methods exhibit comparable S $\cap$ N rates, with CDVAE achieving 4.8% compared to FTCP’s 5.6%. The strong performance of CDVAE in generating novel and stable materials makes it competitive with FTCP in this regard. It is notable, however, that all these rates are lower than the 7.4% achieved by ion exchange, the best-performing baseline method. These results highlight the efficacy of traditional approaches to materials discovery, while also demonstrating the potential of generative models like CDVAE to balance novelty and stability in their outputs.

Despite the reduced S $\cap$ N rates of generative models, they are unique in their ability to generate new structural frameworks that cannot be mapped to any known prototypes. This sets them apart from baseline methods, which rely entirely on existing templates and therefore exhibit 0% prototype novelty rates (**Table 1**). In contrast, the generative models evaluated in this work achieve prototype novelty rates ranging from 6.4% (CrystaLLM) to 16.5% (CDVAE). While none of these structures having novel prototypes are thermodynamically stable (0% prototype S $\cap$ N rates), a considerable fraction of them lies within a reasonably accessible range of metastability. As shown in Supplementary Figure 1, about half of the structures having novel structure prototypes generated from FTCP and CDVAE exhibit  $\Delta E_d < 200$  meV/atom, whereas those from CrystaLLM span a much wider range of energies above the hull. Nevertheless, the lack of structures that are both stable and adopt novel prototypes highlights the need to design generative models that can effectively balance thermodynamic stability with structural novelty.

### Filtering stability with CHGNet

Filtering materials using uMLIPs (*e.g.*, CHGNet)<sup>28</sup> provides a computationally efficient way to improve the stability rate of generation campaigns. Unlike DFT calculations, which are time-consuming and resource-intensive, CHGNet can be used to estimate the internal energy of a material within seconds. This energy can then be compared with a database of DFT-calculated energies to approximate thermodynamic stability. The efficiency of this method allows it to be integrated with any method for generating new materials, whether it be a baseline or generative model. In **Figure 2**, we compare the cumulative distribution functions (CDFs) of DFT-calculated stability results with (left) and without CHGNet filtering (right). In the left panel, the first 500 unique materials generated by each method were computed with DFT and compared to the MP

convex hull. In the right panel, the first 500 unique materials generated by each method that are predicted to be thermodynamically stable using CHGNet were computed with DFT and compared to the MP convex hull.

The unfiltered results in the left panel of **Figure 2** provide a baseline comparison of each method’s ability to generate stable materials (these are CDFs of the same histograms shown in **Figure 1**). As observed in the previous section, ion exchange and FTCP perform best in generating materials that are either stable or close to the convex hull. The similarity of their CDF curves further supports the comparable strengths of these methods. Ion exchange leverages known structural templates and compositional analogies, while FTCP benefits from its latent space sampling strategy that biases generation toward stable regions. In contrast, CDVAE produces materials with more moderate stability. This is reflected by a slower rise in its curve with increasing energy above the hull. Both random enumeration and CrystaLLM are less effective in generating materials close to the hull, as their CDFs exhibit relatively low values until high energies ( $\Delta E_d > 250$  meV/atom) are reached, suggesting a majority of the materials produced by these two methods are unlikely to be accessed experimentally.<sup>48,49</sup>

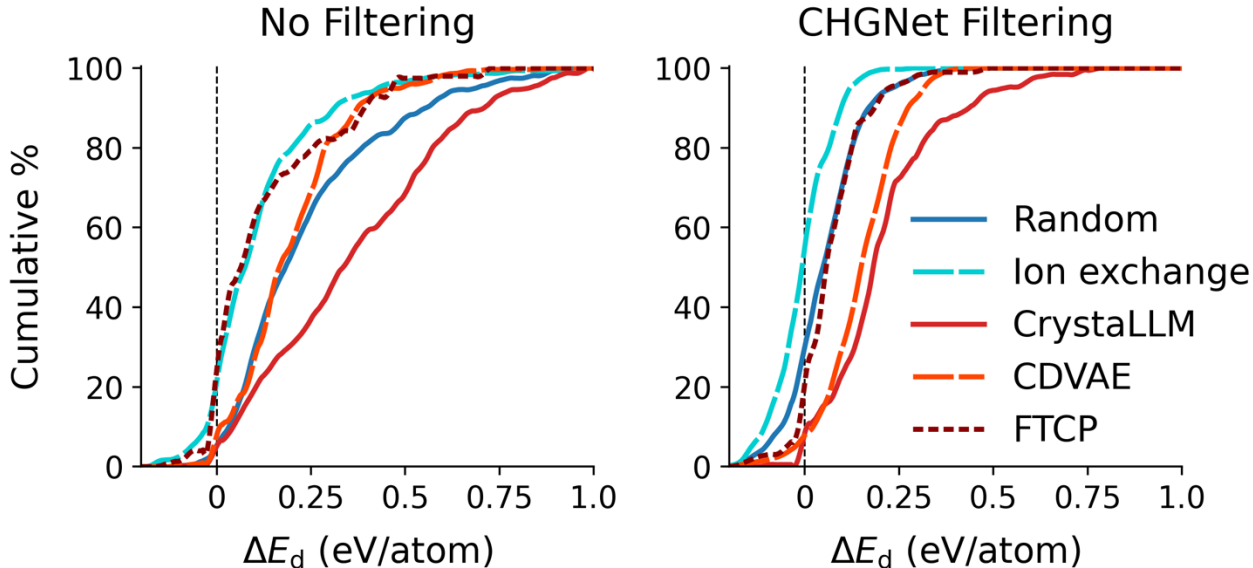


**Figure 2:** Cumulative distribution functions (CDFs) showing the percentage of materials that satisfy a decomposition energy ( $\Delta E_d$ ) cutoff, with each line color-coded by the method used to generate these materials. The left panel displays CDFs for materials generated directly by each method, including two baseline approaches (random enumeration and ion exchange) shaded in blue and three generative models (CrystaLLM, CDVAE, and FTCP) shaded in red. The right panel displays CDFs for materials

filtered by CHGNet-predicted stability, including only those CHGNet predicts to have  $\Delta E_d \leq 0$ . Filtered energy distributions are also displayed in Supplementary Figure 2. Each CDF corresponds with 500 generated structures.

The right panel of **Figure 2** highlights the beneficial effect of CHGNet filtering, which substantially improves the stability of materials generated by most methods as indicated by the leftward shift in all CDFs. The CDF for ion exchange after filtering demonstrates an exceptionally high stability rate of 51.8%, rising steeply and reaching 100% at  $\Delta E_d < 200$  meV/atom. Random enumeration also exhibits improvement, with its curves showing a steeper rise compared to the unfiltered results. By contrast, CDVAE and CrystaLLM show only small improvements after filtering, as evidenced by their shallower curves in the right panel. We speculate that this is due to their tendency to generate materials outside of CHGNet’s training distribution – for example, in under-sampled chemistries or structures that are far out-of-equilibrium – potentially reducing the accuracy of stability predictions and limiting their performance gains. Indeed, Supplementary Figure 3 shows the mean absolute error (MAE) from CHGNet is largest on structures generated by CDVAE and CrystaLLM.

**Table 2** summarizes the results of CHGNet filtering for materials generated by each method. This table includes three metrics: the filter acceptance rate, which indicates the percentage of materials from each method predicted to be stable; the filtered stability rate, representing the percentage of these materials that were confirmed as stable through DFT calculations; and the filtered  $S \cap N$  rate, which measures the percentage of filtered materials that are both DFT-stable and novel. Methods with higher initial stability rates (*e.g.*, ion exchange and FTCP) also tend to have higher acceptance rates after filtering. However, the filtered stability rates remain consistently well below 100% for all methods, with ion exchange achieving the highest rate of 51.8%. This indicates that CHGNet tends to over-predict the stability of generated candidates, as all materials passing through the filter are predicted to be stable using CHGNet energies. This over-prediction likely arises because CHGNet (like most uMLIPs) was trained primarily on compounds near the convex hull, biasing its predictions toward stability.<sup>50–52</sup> The bias is most evident in CrystaLLM and CDVAE, where filtered stability rates are the lowest (9.0% and 8.9%), likely due to their generated materials lying far outside CHGNet’s training distribution.

The filtered  $S \cap N$  rate offers additional insights by assessing both stability and novelty. Interestingly, random enumeration combined with CHGNet achieves the highest filtered  $S \cap N$  rate

(27.7%), surpassing ion exchange (18.1%) despite the latter’s superior filtered stability rate. This is because many materials generated *via* ion exchange already exist in MP, reducing their novelty. In contrast, random enumeration generates a broader range of compositions, enabling it to identify stable and novel materials after CHGNet filtering. While the high performance of random enumeration on S $\cap$ N after filtering is interesting, it should be noted that material novelty could have been added as a filter early in the generation process, in which case the stability rate reported in **Table 2** would approximate the S $\cap$ N rate.

**Table 2:** Metrics for CHGNet filtering of materials generated by two baseline methods and three generative models. The filter acceptance rate indicates the percentage of materials from each method predicted to be stable by CHGNet. The filtered stability rate corresponds to the percentage of these CHGNet-predicted stable materials that were confirmed as stable through density functional theory (DFT) calculations. The filtered S $\cap$ N rate reflects the percentage of materials that are both DFT-stable and novel, meaning their composition and structure are not already present in the Materials Project. Statistics for filtered stability rate and filtered S $\cap$ N rate are based on 500 structures for Random, Ion exchange, and FTCP and 300 structures for CrystaLLM and CDVAE.

Method	Filter acceptance rate	Filtered stability rate	Filtered S $\cap$ N rate
Random	5.2%	31.8%	<b>27.7%</b>
Ion exchange	<b>48.8%</b>	<b>51.8%</b>	18.1%
CrystaLLM	8.6%	9.0%	8.6%
CDVAE	12.0%	8.9%	8.2%
FTCP	40.9%	19.4%	3.4%

### Generating materials with targeted properties

Beyond generating thermodynamically stable materials, it is also useful to generate materials with targeted properties for particular applications. We first evaluated four distinct approaches for generating materials with a band gap near 3 eV. Two baseline methods were tested: random enumeration and ion exchange. Additionally, we applied ML filtering (based on predictions from CGCNN)<sup>29</sup> to the randomly enumerated materials to assess its impact on targeting specific properties. Finally, we tested one generative model, FTCP, which was chosen due to its ability to condition its latent space on specific properties and its superior performance among the

generative models in producing stable materials. A total of 500 structures were generated from each method, and the distributions of their DFT-computed band gaps are shown in **Figure 3**.

Random enumeration produced a wide variety of materials, with 42.1% of them being metallic. Only 9.2% of the generated materials exhibited a band gap within 0.5 eV of the desired value (3 eV), demonstrating the low success rate of computational screening when no guidance is provided. Applying CGCNN to filter these randomly enumerated materials improved the results considerably. By only retaining materials with CGCNN-predicted band gaps near 3 eV, the proportion of metals dropped to 16.1%, and 24.6% of the filtered materials exhibited band gaps within 0.5 eV of the target. As with CHGNet-filtering, this showcases the utility of ML-based screening for quickly refining large pools of candidate materials.

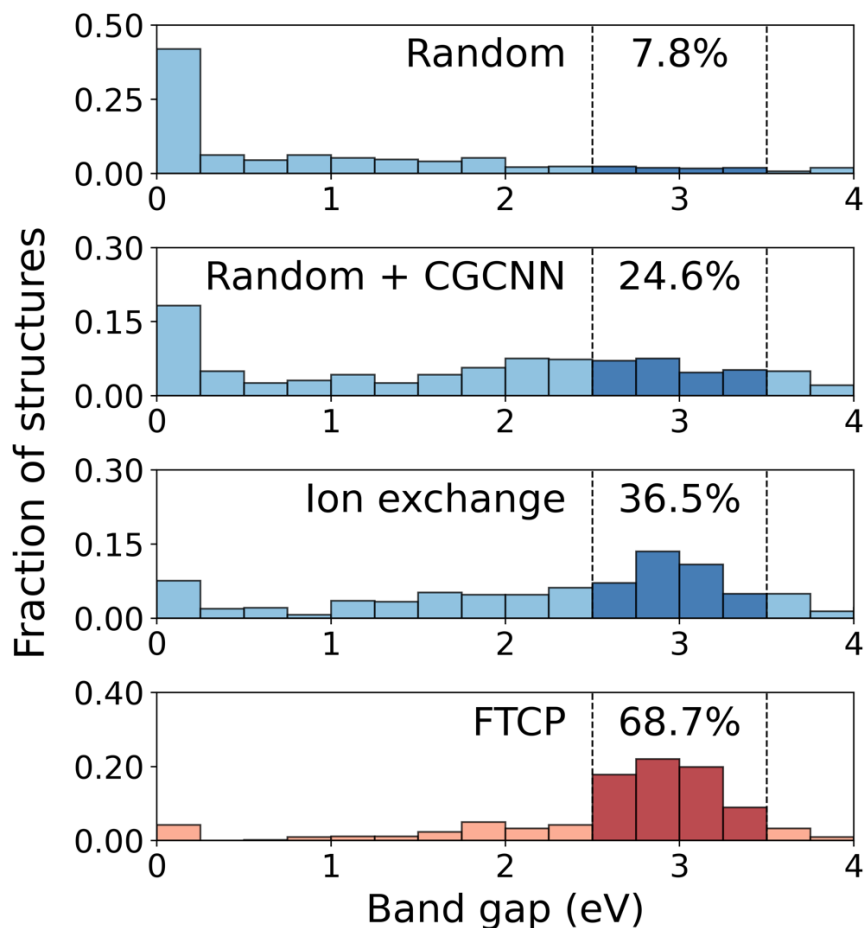


**Figure 3:** Histograms showing density functional theory (DFT) computed band gap distributions of structures generated by two baseline methods (random enumeration and ion exchange, colored blue), CGCNN (also colored blue) applied to filter the randomly enumerated materials, and one generative model: FTCP (colored red). For each of the four approaches, 500 structures were considered. With the

exception of random enumeration, all methods specifically targeted materials with a band gap near 3 eV. The percentage of generated materials with a band gap in the range of 2.5 to 3.5 eV is displayed above the shaded bars in each subplot.

Data-driven ion exchange performed even better than CGCNN filtering of randomly enumerated materials, leveraging its ability to generate hypothetical compounds by substituting ions in known materials from MP that already have band gaps close to 3 eV. This method resulted in only 14.5% metallic materials and a substantial 34.8% of materials with band gaps within 0.5 eV of the target. This strong performance may not be entirely surprising as many of the compositional changes introduced by ion exchange are relatively minor, especially when the substituted element constitutes a small fraction of the overall chemical formula. This mirrors our findings from the previous section, highlighting the tradeoff between achieving success – whether in targeted properties or stability – and prioritizing novelty or diversity in the generated structures.

FTCP outperformed all other methods in targeting electronic band gap, with 67.3% of its generated materials exhibiting a band gap within 0.5 eV of the desired value (3 eV). This success likely stems from FTCP’s ability to sample from a latent space informed by known compounds with the band gaps close to the target, enabling the generation of materials with structural or compositional similarities to the reference points. Importantly, this is accomplished while retaining a large proportion of stable materials: 22.4% of those generated by FTCP exhibit  $\Delta E_d \leq 0$ , and many more lie reasonably close to the convex hull (Supplementary Figure 4). This result suggests that generative models can excel in targeted property generation, outperforming the baseline methods, while maintaining relatively high stability rates.

Using the same four methods described above (for targeting a desired band gap), we next generated materials with the objective of maximizing bulk modulus. This task fundamentally differs from the previous band gap-related objective by focusing on materials with extreme properties (*e.g.*, maximal bulk modulus) instead of those within an intermediate range (*e.g.*, band gaps near 3 eV). A total of 500 materials were sampled from each method, and their bulk moduli were computed using Birch-Murnaghan equations of state fit to DFT-computed energies. The resulting distributions of bulk moduli are shown in **Figure 4**. Materials generated through random enumeration follow a Poisson-like distribution of bulk moduli with a peak near 50–60 GPa, closely resembling the known distribution of elastic properties for materials in MP.<sup>53</sup> If we define success

as finding materials with a bulk modulus  $\geq 300$  GPa, then random enumeration achieves this at a rate of only 4.2%. When CGCNN is applied to filter these materials, it causes a noticeable shift in the distribution toward higher bulk moduli, and 16.9% of the filtered materials exhibit a bulk modulus  $\geq 300$  GPa.

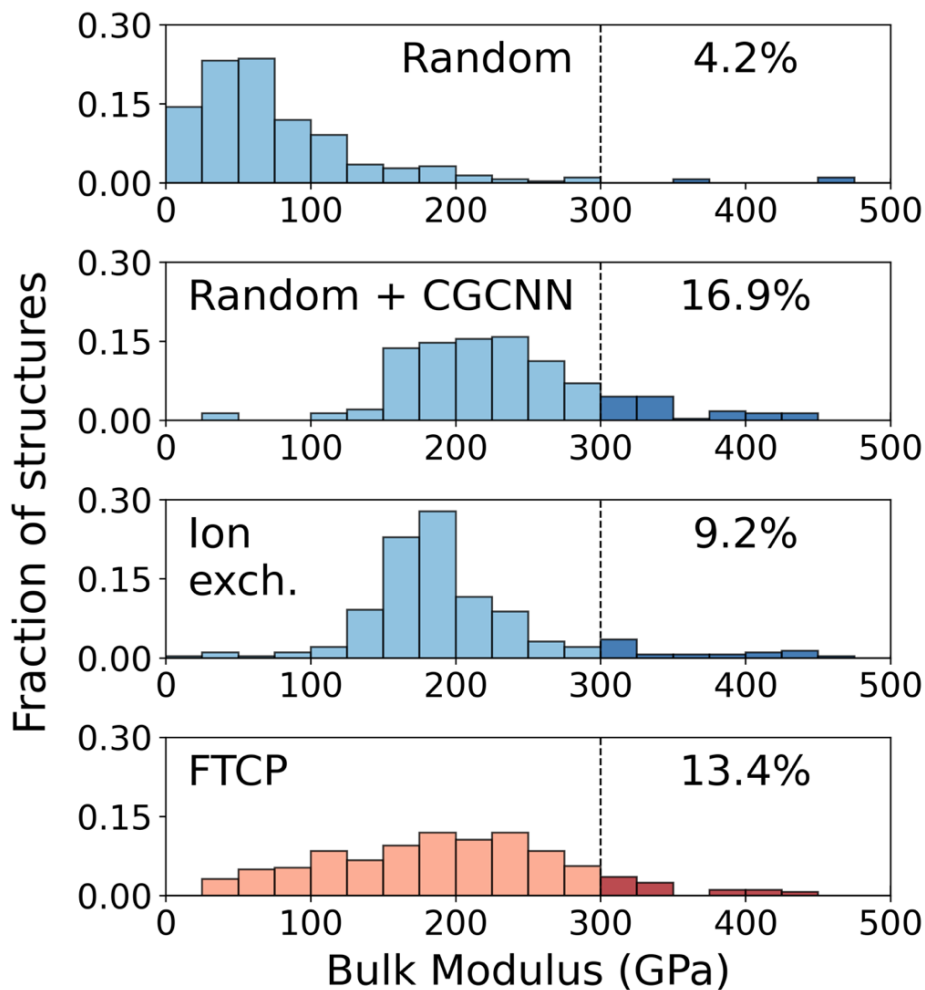


**Figure 4:** Histograms showing density functional theory (DFT) computed bulk moduli distributions of structures generated by two baseline methods (random enumeration and ion exchange, colored blue), CGCNN (also colored blue) applied to filter the randomly enumerated materials, and one generative model: FTCP (colored red). For each of the four approaches, 500 structures were considered. With the exception of random enumeration, all methods specifically targeted materials with a bulk modulus  $\geq 300$  GPa. The percentage of generated materials satisfying this objective is displayed above the shaded bars in each subplot.



When applied to known materials in MP with high bulk moduli, ion exchange performs more modestly, with 9.2% of the resulting materials exhibiting a bulk modulus  $\geq 300$  GPa. This smaller shift in the distribution likely reflects the tendency for ion exchange to introduce only minor compositional changes, which limits its ability to substantially alter the mechanical properties of the original materials – many of which (in MP) do not exhibit anomalously high bulk moduli. FTCP performed better than ion exchange but worse than ML filtering of randomly enumerated materials, with 13.4% of the compounds generated by FTCP exhibiting a bulk modulus  $\geq 300$  GPa. Compared to its strong performance on electronic band gap, we suspect FTCP is less effective here given the scarcity of materials with extremely high bulk moduli in MP. This lack of training data may limit the conditioning of the autoencoder’s latent space on extreme bulk modulus values. Nevertheless, FTCP still has an advantage in generating stable materials while maximizing bulk modulus. In comparison to filtering of randomly enumerated materials using CGCNN, where only 0.8% of the resulting compounds are stable ( $\Delta E_d \leq 0$ ), FTCP maintains a much higher stability rate of 17.1% during this targeted property generation (Supplementary Figure 5). This again points to the relative strength of generative models in considering both stability and properties while proposing new materials. Yet these relatively low percentages from even the best methods further highlight the challenge of identifying “exceptional” materials, as the inherent scarcity of analogs in the materials space and limited training data inhibit the development of effective models for both generation and filtering.<sup>54</sup> It should also be noted that ion exchange achieves stability rates in the vicinity of FTCP for both property prediction tasks (26.1% for the band gap task and 11.9% for bulk modulus), reinforcing that traditional approaches provide a competitive baseline for comparison.

## Discussion

The recent surge in generative models for inorganic crystalline materials underscores the growing need for benchmarks to assess their performance. While metrics such as stability and novelty provide valuable insight, there is a lack of clear baselines for comparison. To address this gap, we developed and evaluated two baseline methods: random enumeration of charge-balanced compositions in known structure prototypes, and targeted ion substitution of known materials with desired properties. These approaches leverage existing data from AFLOW<sup>26,27</sup> and the Materials Project,<sup>23</sup> which offer a wealth of information on structure prototypes and calculated properties

acquired from DFT calculations. They also benefit from simple yet powerful chemical heuristics; charge balance favors validity of proposed chemical formulae, and substitutions are performed on ions of comparable size and oxidation state. As a result, the baseline methods perform surprisingly well in generating stable materials not found in existing databases. Random enumeration achieves a stable and novel ( $S \cap N$ ) rate of 3.8%, while ion exchange achieves an even higher rate of 7.4%. There remains ample opportunity to further increase these rates as additional chemical heuristics are introduced to better filter computationally proposed materials.<sup>55</sup>

The strong performance of the baseline methods establishes a high benchmark for generative models to meet or exceed. For this task, we tested a variational autoencoder (FTCP),<sup>11</sup> a large-language model (CrystaLLM),<sup>14</sup> and a diffusion model (CDVAE).<sup>12</sup> Our tests showed FTCP to be most effective in generating stable materials, achieving a high stability rate of 26.8%. However, many of these materials were found to already exist in the Materials Project, bringing the  $S \cap N$  rate to 5.6% – notably lower than ion exchange. On the other hand, CDVAE excels in generating materials with a high degree of structural novelty (at a slightly lower  $S \cap N$  rate of 4.8%), with 16.5% of generated materials unable to be mapped to any known structure prototype in the AFLOW database. The capability of generating entirely new structural arrangements is unique to the generative models, whereas the baseline methods rely on known structural templates for ion substitution.

Generative models also perform well in targeting specific material properties when sufficient training data is available. For instance, FTCP achieves a high success rate of 67.5% in generating materials with a desired band gap near 3 eV, far surpassing the 34.8% achieved by ion exchange. This performance diminishes when targeting extreme values of properties such as high bulk moduli (> 300 GPa) that are less well represented in the training set. However, FTCP retains a higher stability rate than the baseline methods during targeted property generation, an important advantage when searching for materials that not only exhibit desired properties but also have a good chance to be synthesized experimentally.

To enhance the performance of the methods discussed in this paper, machine learning models were used to filter proposed materials based on predicted thermodynamic stability or desired properties. Our results demonstrate that this is a highly effective approach. For instance, filtering by predicted stability using a pre-trained uMLIP (CHGNet)<sup>28</sup> substantially improves the stability rates of generated materials. For instance, a high 51.8% of materials generated through

ion exchange lie on the DFT convex hull after CHGNet filtering. This rate decreases for some of the generative models such as CDVAE and CrystaLLM, which produce more novel materials that likely fall outside of CHGNet’s training distribution. As the breadth and diversity of training data for uMLIPs improves,<sup>56</sup> this should prove to be an even more effective approach to filter the results of generative models.

Similar findings were observed when using a pre-trained graph neural network (CGCNN)<sup>29</sup> to filter materials by predicted band gap and bulk modulus. Doing so leads to a near three-fold increase in the success rate of identifying materials with desired properties compared to random enumeration but remains relatively low (16.9%) when targeting extreme property values (*e.g.*, a bulk modulus > 300 GPa). It also leads to a decrease in the stability rate of the proposed materials, though incorporating a uMLIP-based stability filter could mitigate this issue. As with uMLIPs, these findings underscore the need to broaden and diversify training data for property prediction models to enhance the efficiency of generative approaches in identifying novel materials with exceptional properties.

Our findings demonstrate that there is still room for improvement in the design of generative models for inorganic materials, particularly when they are used to find new materials that are thermodynamically stable. To streamline the development of future models, we provide all of the data and code from this work in a publicly accessible GitHub repository (see Data Availability Statement). We envision these resources being used for benchmarking generative models and integrating them with traditional screening methods to enhance the success rate in discovering new materials that are likely to be synthesized and display desired properties.

### **Data Availability Statement**

The code for generating materials through random enumeration and ion exchange is available at [https://github.com/Bartel-Group/matgen\\_baselines](https://github.com/Bartel-Group/matgen_baselines). This repository also includes code for machine learning filtering using CHGNet and pre-trained checkpoints for the generative models discussed here.

### **Acknowledgements**

The authors gratefully acknowledge support from the University of Minnesota in the form of new faculty start-up. The authors also acknowledge the Minnesota Supercomputing Institute (MSI) at the University of Minnesota for providing resources that contributed to the research

results reported herein. This work was also enabled by the dedication and open-source contributions of prior developers, including those behind the pre-trained graph neural networks (CHGNet and CGCNN), generative models (CrystaLLM, CDVAE, and FTCP), pymatgen (DMSP), and AFLOW (structure prototypes).

## References

1. Cheetham, A. K., Seshadri, R. & Wudl, F. Chemical synthesis and materials discovery. *Nat. Synth* **1**, 514–520 (2022).
2. A. Manthiram, J. C. Knight, S.-T. Myung, S.-M. Oh, & Y.-K. Sun. Nickel-Rich and Lithium-Rich Layered Oxide Cathodes: Progress and Perspectives. *Adv. Energy Mater.* **6**, 1501010 (2016).
3. K. Nomura *et al.* Thin-Film Transistor Fabricated in Single-Crystalline Transparent Oxide Semiconductor. *Science* **300**, 1269–1272 (2003).
4. K. M. Shen & J. C. Seamus Davis. Cuprate high-T<sub>c</sub> superconductors. *Mater. Today* **11**, 14–21 (2008).
5. Park, H., Li, Z. & Walsh, A. Has generative artificial intelligence solved inverse materials design? *Matter* **7**, 2355–2367 (2024).
6. A. Noura, N. Sokolovska, & J.-C. Crivello. CrystalGAN: Learning to Discover Crystallographic Structures with Generative Adversarial Networks. *arXiv:1810.11203* (2018).
7. S. Kim, J. Noh, G. Gu, A. Aspuru-Guzik, & Y. Jung. Generative Adversarial Networks for Crystal Structure Prediction. *ACS Cent. Sci.* **6**, 1412–1420 (2020).
8. Y. Zhao *et al.* High-Throughput Discovery of Novel Cubic Crystal Materials Using Deep Generative Neural Networks. *Adv. Sci.* **8**, 2100566 (2021).
9. J. Noh *et al.* Inverse Design of Solid-State Materials via a Continuous Representation. *Matter* **1**, 1370–1384 (2019).
10. Court, C. J., Yildirim, B., Jain, A. & Cole, J. M. 3-D Inorganic Crystal Structure Generation and Property Prediction via Representation Learning. *J. Chem. Inf. Model.* **60**, 4518–4535 (2020).
11. Ren, Z. *et al.* An invertible crystallographic representation for general inverse design of inorganic crystals with targeted properties. *Matter* **5**, 314–335 (2022).
12. Xie, T., Fu, X., Ganea, O.-E., Barzilay, R. & Jaakkola, T. Crystal Diffusion Variational Autoencoder for Periodic Material Generation. Preprint at <https://doi.org/10.48550/arXiv.2110.06197> (2022).
13. Zhu, R., Nong, W., Yamazaki, S. & Hippalgaonkar, K. WyCryst: Wyckoff inorganic crystal generator framework. *Matter* **7**, 3469–3488 (2024).

14. Antunes, L. M., Butler, K. T. & Grau-Crespo, R. Crystal Structure Generation with Autoregressive Large Language Modeling. Preprint at <https://doi.org/10.48550/arXiv.2307.04340> (2024).
15. Flam-Shepherd, D. & Aspuru-Guzik, A. Language models can generate molecules, materials, and protein binding sites directly in three dimensions as XYZ, CIF, and PDB files. Preprint at <https://doi.org/10.48550/arXiv.2305.05708> (2023).
16. Gruver, N. *et al.* Fine-Tuned Language Models Generate Stable Inorganic Materials as Text. Preprint at <https://doi.org/10.48550/arXiv.2402.04379> (2024).
17. Alverson, M. *et al.* Generative adversarial networks and diffusion models in material discovery. *Digital Discovery* **3**, 62–80 (2024).
18. Jiao, R. *et al.* Crystal Structure Prediction by Joint Equivariant Diffusion. Preprint at <https://doi.org/10.48550/arXiv.2309.04475> (2024).
19. Zeni, C. *et al.* MatterGen: a generative model for inorganic materials design. Preprint at <https://doi.org/10.48550/arXiv.2312.03687> (2024).
20. Yang, S. *et al.* Scalable Diffusion for Materials Generation. Preprint at <https://doi.org/10.48550/arXiv.2311.09235> (2024).
21. Miller, B. K., Chen, R. T. Q., Sriram, A. & Wood, B. M. FlowMM: Generating Materials with Riemannian Flow Matching. Preprint at <https://doi.org/10.48550/arXiv.2406.04713> (2024).
22. Sriram, A., Miller, B. K., Chen, R. T. Q. & Wood, B. M. FlowLLM: Flow Matching for Material Generation with Large Language Models as Base Distributions. Preprint at <https://doi.org/10.48550/arXiv.2410.23405> (2024).
23. A. Jain *et al.* Commentary: The Materials Project: A materials genome approach to accelerating materials innovation. *APL Mater.* **1**, 011002 (2013).
24. Baird, S. G., Sayeed, H. M., Montoya, J. & Sparks, T. D. matbench-genmetrics: A Python library for benchmarking crystal structure generative models using time-based splits of Materials Project structures. *Journal of Open Source Software* **9**, 5618 (2024).
25. Riebesell, J. *et al.* Matbench Discovery -- A framework to evaluate machine learning crystal stability predictions. Preprint at <https://doi.org/10.48550/arXiv.2308.14920> (2024).
26. Mehl, M. J. *et al.* The AFLOW Library of Crystallographic Prototypes: Part 1. *Computational Materials Science* **136**, S1–S828 (2017).
27. Hicks, D. *et al.* The AFLOW Library of Crystallographic Prototypes: Part 2. *Computational Materials Science* **161**, S1–S1011 (2019).
28. B. Deng *et al.* CHGNet as a pretrained universal neural network potential for charge-informed atomistic modelling. *Nat. Mach. Intell.* **5**, 1031–1041 (2023).
29. T. Xie & J. C. Grossman. Crystal Graph Convolutional Neural Networks for an Accurate and Interpretable Prediction of Material Properties. *Phys. Rev. Lett.* **120**, 145301 (2018).

30. S. P. Ong *et al.* Python Materials Genomics (pymatgen): A robust, open-source python library for materials analysis. *Comput. Mater. Sci.* **68**, 314–319 (2013).
31. Hautier, G., Fischer, C., Ehrlicher, V., Jain, A. & Ceder, G. Data Mined Ionic Substitutions for the Discovery of New Compounds. *Inorg. Chem.* **50**, 656–663 (2011).
32. Levin, I. NIST Inorganic Crystal Structure Database (ICSD). National Institute of Standards and Technology <https://doi.org/10.18434/M32147> (2020).
33. Perdew, J. P., Burke, K. & Ernzerhof, M. Generalized Gradient Approximation Made Simple. *Phys. Rev. Lett.* **77**, 3865–3868 (1996).
34. Kresse, G. & Furthmüller, J. Efficiency of ab-initio total energy calculations for metals and semiconductors using a plane-wave basis set. *Computational Materials Science* **6**, 15–50 (1996).
35. Kresse, G. & Furthmüller, J. Efficient iterative schemes for ab initio total-energy calculations using a plane-wave basis set. *Phys. Rev. B* **54**, 11169–11186 (1996).
36. C. J. Bartel. Review of computational approaches to predict the thermodynamic stability of inorganic solids. *J. Mater. Sci.* **57**, 10475–10498 (2022).
37. Wang, A. *et al.* A framework for quantifying uncertainty in DFT energy corrections. *Sci Rep* **11**, 15496 (2021).
38. Birch, F. Finite Elastic Strain of Cubic Crystals. *Phys. Rev.* **71**, 809–824 (1947).
39. Larsen, A. H. *et al.* The atomic simulation environment—a Python library for working with atoms. *J. Phys.: Condens. Matter* **29**, 273002 (2017).
40. Zhang, X., Stevanović, V., d’Avezac, M., Lany, S. & Zunger, A. Prediction of  $A_2B_4X_4$  metal-chalcogenide compounds via first-principles thermodynamics. *Phys. Rev. B* **86**, 014109 (2012).
41. Davies, D. W. *et al.* Computational Screening of All Stoichiometric Inorganic Materials. *Chem* **1**, 617–627 (2016).
42. Gorai, P., Ganose, A., Faghaninia, A., Jain, A. & Stevanović, V. Computational discovery of promising new n-type dopable ABX<sub>3</sub> Zintl thermoelectric materials. *Mater. Horiz.* **7**, 1809–1818 (2020).
43. Vasylenko, A. *et al.* Element selection for crystalline inorganic solid discovery guided by unsupervised machine learning of experimentally explored chemistry. *Nat Commun* **12**, 5561 (2021).
44. Merchant, A. *et al.* Scaling deep learning for materials discovery. *Nature* **624**, 80–85 (2023).
45. S. Kirklin *et al.* The Open Quantum Materials Database (OQMD): assessing the accuracy of DFT formation energies. *npj Comput. Mater.* **1**, 15010 (2015).
46. C. Draxl & M. Scheffler. The NOMAD laboratory: from data sharing to artificial intelligence. *J. Phys.: Mater.* **2**, 036001 (2019).

47. T. Butler, K., M. Frost, J., M. Skelton, J., L. Svane, K. & Walsh, A. Computational materials design of crystalline solids. *Chemical Society Reviews* **45**, 6138–6146 (2016).
48. W. Sun *et al.* The thermodynamic scale of inorganic crystalline metastability. *Sci. Adv.* **2**, e160022 (2016).
49. M. Aykol, S. S. Dwaraknath, W. Sun, & K. A. Persson. Thermodynamic limit for synthesis of metastable inorganic materials. *Sci. Adv.* **4**, eaaq014 (2018).
50. Bartel, C. J. *et al.* A critical examination of compound stability predictions from machine-learned formation energies. *npj Comput Mater* **6**, 1–11 (2020).
51. Arróyave, R. Phase Stability Through Machine Learning. *J. Phase Equilib. Diffus.* **43**, 606–628 (2022).
52. Deng, B. *et al.* Overcoming systematic softening in universal machine learning interatomic potentials by fine-tuning. Preprint at <https://doi.org/10.48550/arXiv.2405.07105> (2024).
53. de Jong, M. *et al.* Charting the complete elastic properties of inorganic crystalline compounds. *Sci Data* **2**, 150009 (2015).
54. Schrier, J., Norquist, A. J., Buonassisi, T. & Brgoch, J. In Pursuit of the Exceptional: Research Directions for Machine Learning in Chemical and Materials Science. *J. Am. Chem. Soc.* **145**, 21699–21716 (2023).
55. Das, B., Ji, K., Sheng, F., McCall, K. M. & Buonassisi, T. Embedding human knowledge in material screening pipeline as filters to identify novel synthesizable inorganic materials. *Faraday Discuss.* (2024) doi:10.1039/D4FD00120F.
56. Barroso-Luque, L. *et al.* Open Materials 2024 (OMat24) Inorganic Materials Dataset and Models. Preprint at <https://doi.org/10.48550/arXiv.2410.12771> (2024).
57. Neumann, M. *et al.* Orb: A Fast, Scalable Neural Network Potential. Preprint at <https://doi.org/10.48550/arXiv.2410.22570> (2024).
58. Park, Y., Kim, J., Hwang, S. & Han, S. Scalable Parallel Algorithm for Graph Neural Network Interatomic Potentials in Molecular Dynamics Simulations. Preprint at <http://arxiv.org/abs/2402.03789> (2024).
59. Batatia, I. *et al.* A foundation model for atomistic materials chemistry. Preprint at <https://doi.org/10.48550/arXiv.2401.00096> (2024).

**Supplementary Information**  
**Establishing baselines for generative discovery of inorganic crystals**

Nathan J. Szymanski<sup>1</sup> and Christopher J. Bartel<sup>1,\*</sup>

**Table of contents**

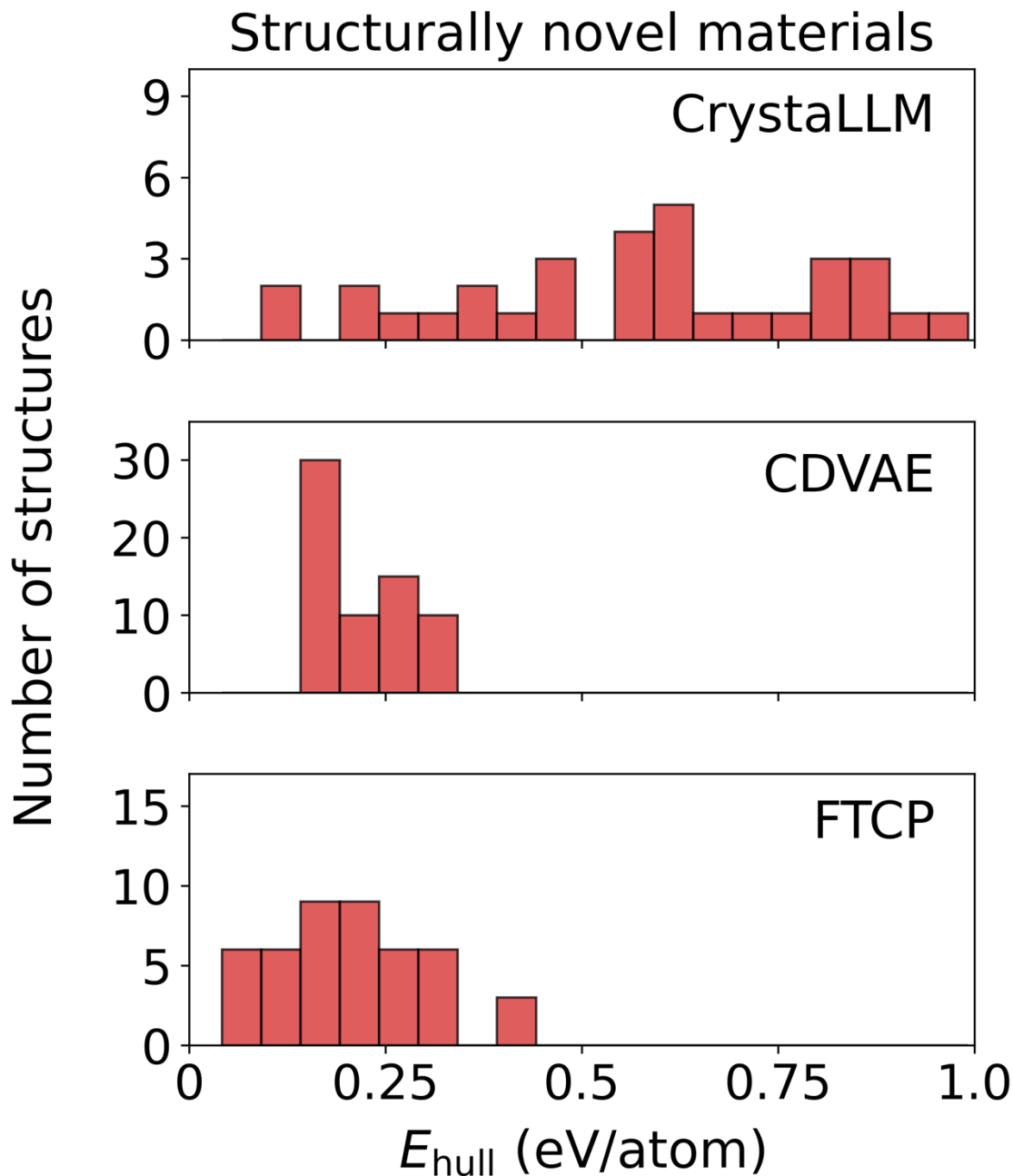
Supplementary Figures 1-5

---

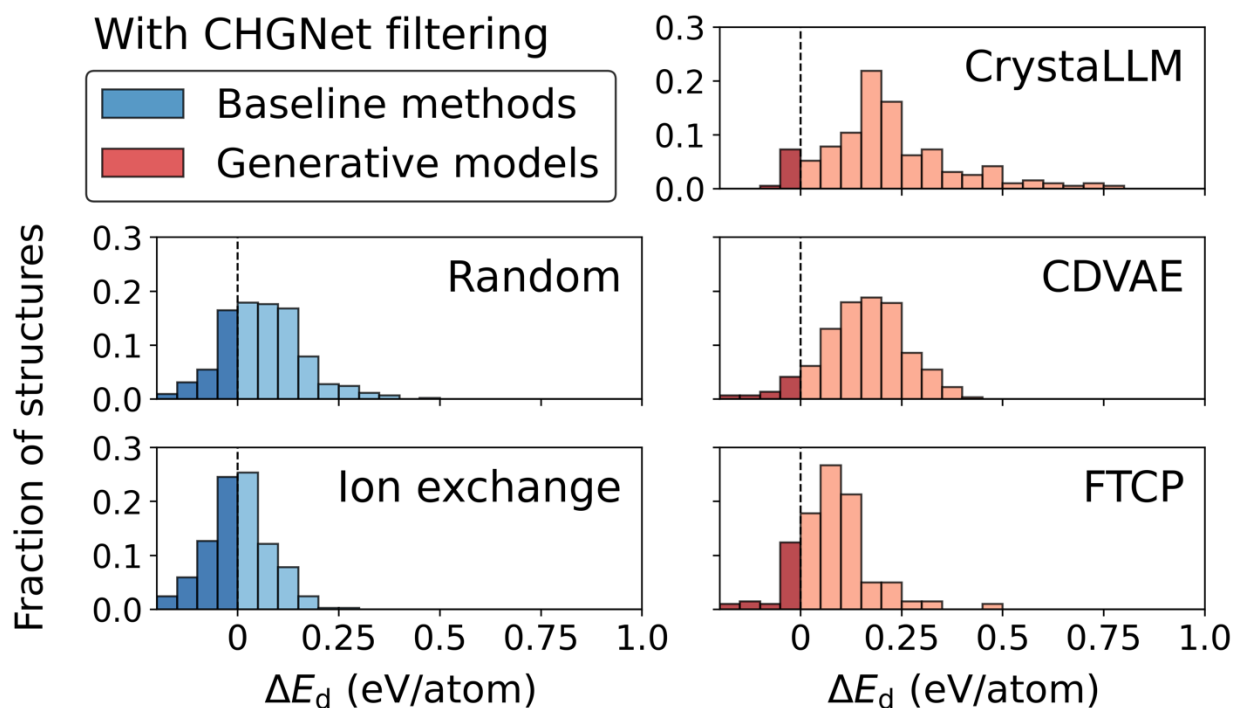
<sup>1</sup> University of Minnesota, Department of Chemical Engineering and Materials Science, Minneapolis, MN, USA 55455

\* Correspondence to [cbartel@umn.edu](mailto:cbartel@umn.edu)

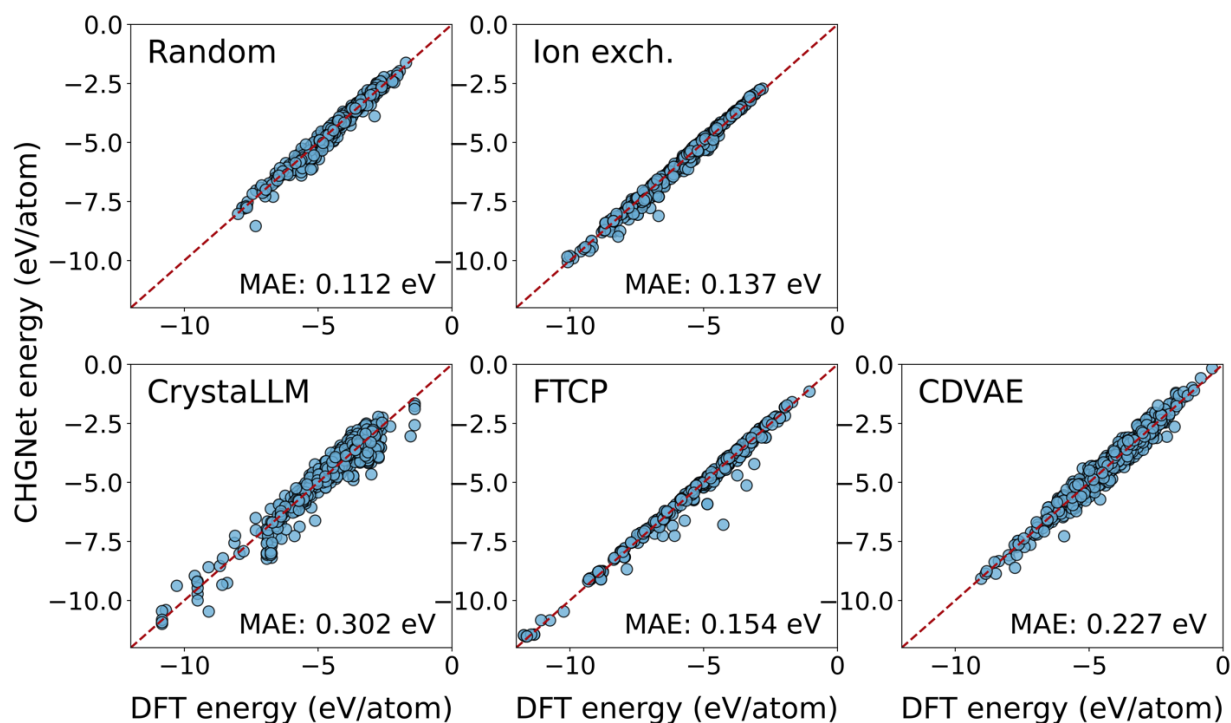




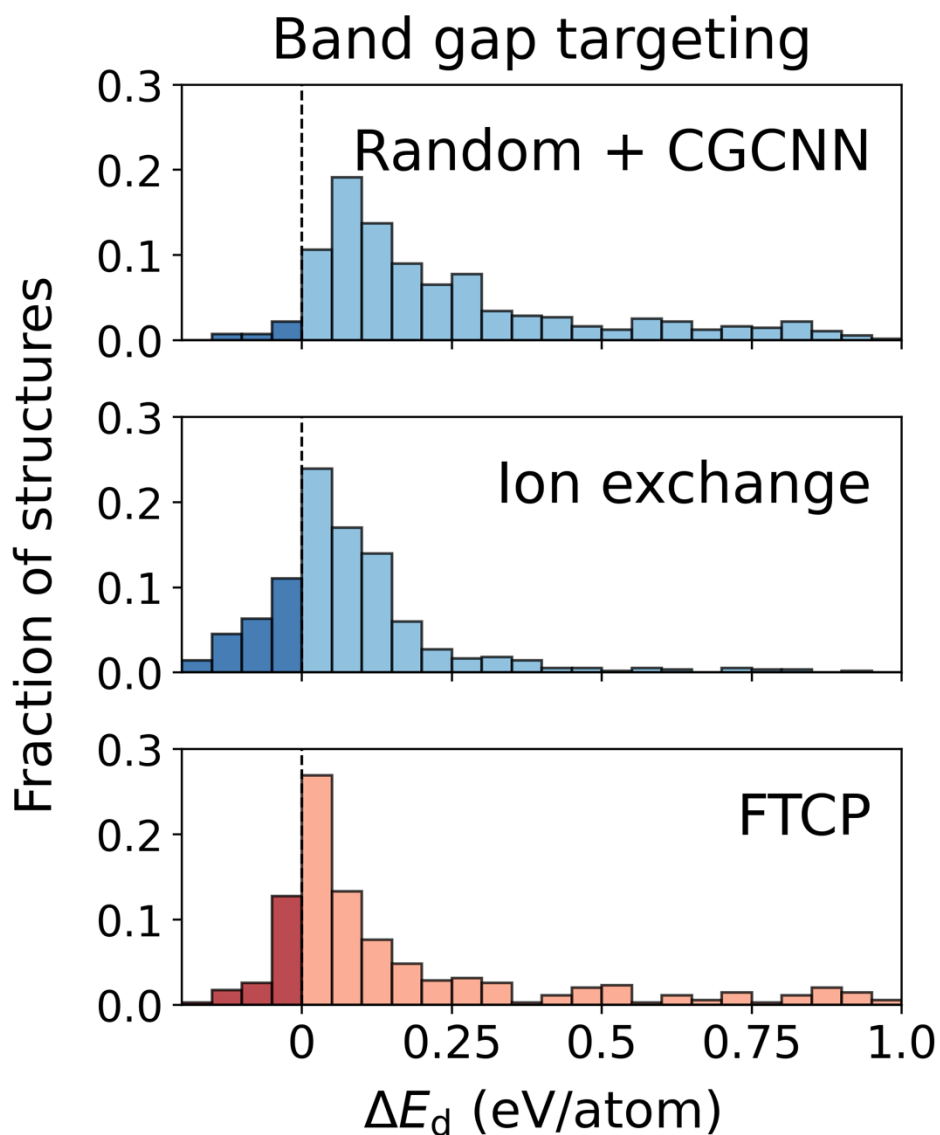
**Supplementary Figure 1:** Histograms showing density functional theory (DFT) computed energies above the convex hull for all the *structurally novel* compounds – meaning they cannot be mapped to known structure prototypes in the AFLOW database – created by three different generative models: CrystaLLM,<sup>1</sup> FTCP,<sup>2</sup> and CDVAE.<sup>3</sup>



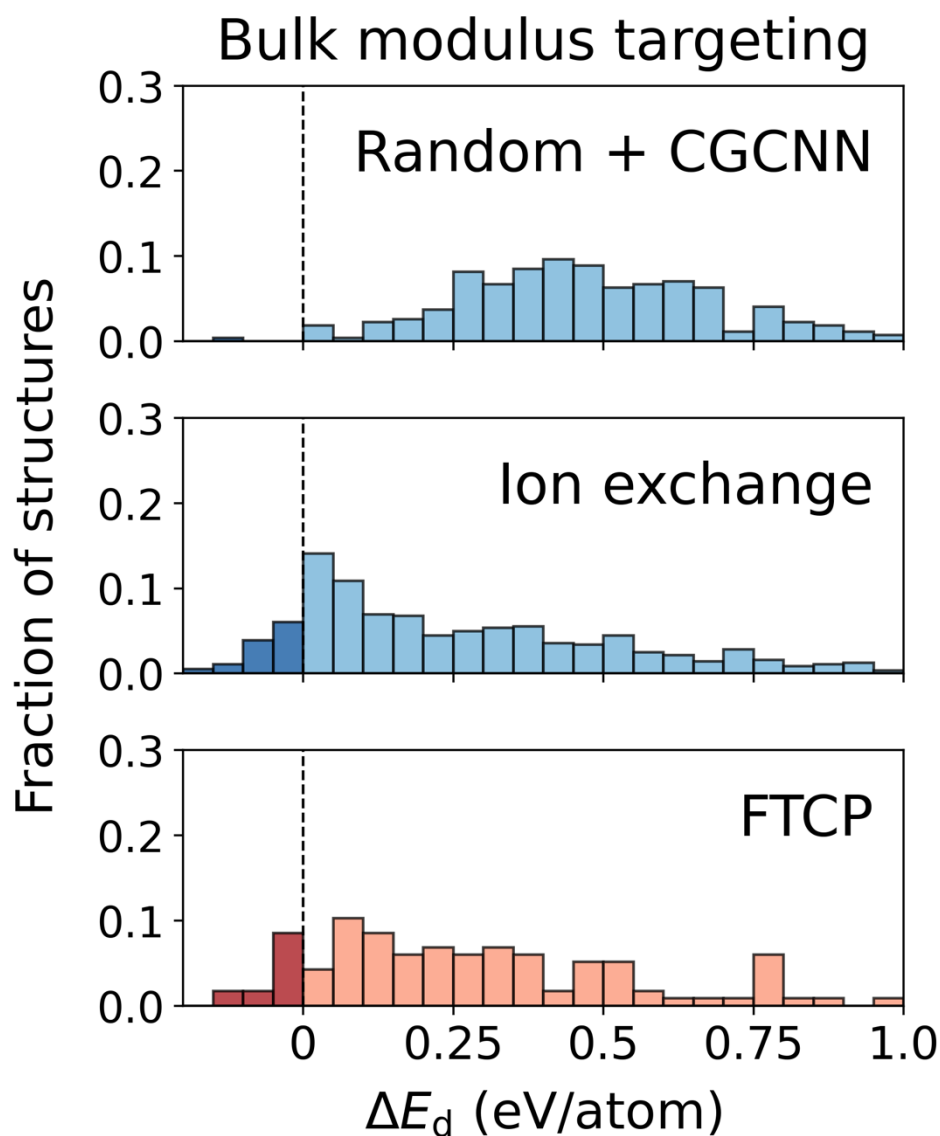
**Supplementary Figure 2:** Histograms showing DFT-computed decomposition energies ( $\Delta E_d$ ) for structures that were filtered by CHGNet-predicted stability<sup>4</sup>. These include structures generated by two baseline methods and three generative models. For each of the five approaches, 500 structures were considered. The left column (colored blue) contains results from the baseline methods: random enumeration and ion exchange. The right column (colored red) contains results from the generative model: CrystaLLM,<sup>1</sup> FTCP,<sup>2</sup> and CDVAE.<sup>3</sup>



**Supplementary Figure 3:** Scatter plots comparing CHGNet-predicted with DFT-calculated energies of structures generated by two baseline methods (random enumeration and ion exchange) and three generative models: CrystaLLM,<sup>1</sup> FTCP,<sup>2</sup> and CDVAE.<sup>3</sup> Both CHGNet and DFT were given the same starting structure and each relaxed it before computing a final energy. The plotted energies include corrections for anions and GGA/GGA+U mixing.<sup>5</sup> The large mean absolute errors (MAEs) are likely in part caused by the loose convergence criterion (forces were converged below 0.1 eV/Å) we used for CHGNet relaxations compared with DFT relaxations (0.03 eV/Å).



**Supplementary Figure 4:** Histograms showing DFT-computed decomposition energies of structures generated by 1) using CGCNN to filter randomly enumerated materials, 2) data-driven ion exchange, and 3) a generative model, FTCP.<sup>2</sup> These approaches targeted materials with band gap near 3 eV, regardless of whether they are stable. Results from random enumeration are not included here since they follow the same distribution as shown in Figure 1 of the main text.



**Supplementary Figure 5:** Histograms showing DFT-computed decomposition energies of structures generated by 1) using CGCNN<sup>6</sup> to filter randomly enumerated materials, 2) data-driven ion exchange, and 3) a generative model, FTCP.<sup>2</sup> These approaches targeted materials with a high bulk modulus, regardless of whether they are stable. Results from random enumeration are not included here since they follow the same distribution as shown in Figure 1 of the main text.

## References

1. Antunes, L. M., Butler, K. T. & Grau-Crespo, R. Crystal Structure Generation with Autoregressive Large Language Modeling. Preprint at <https://doi.org/10.48550/arXiv.2307.04340> (2024).
2. Ren, Z. *et al.* An invertible crystallographic representation for general inverse design of inorganic crystals with targeted properties. *Matter* **5**, 314–335 (2022).
3. Xie, T., Fu, X., Ganea, O.-E., Barzilay, R. & Jaakkola, T. Crystal Diffusion Variational Autoencoder for Periodic Material Generation. Preprint at <https://doi.org/10.48550/arXiv.2110.06197> (2022).
4. B. Deng *et al.* CHGNet as a pretrained universal neural network potential for charge-informed atomistic modelling. *Nat. Mach. Intell.* **5**, 1031–1041 (2023).
5. Wang, A. *et al.* A framework for quantifying uncertainty in DFT energy corrections. *Sci Rep* **11**, 15496 (2021).
6. T. Xie & J. C. Grossman. Crystal Graph Convolutional Neural Networks for an Accurate and Interpretable Prediction of Material Properties. *Phys. Rev. Lett.* **120**, 145301 (2018).